IMPLEMENTATION OF A PASSIVE DEHUMIDIFICATION SYSTEM BASED ON FOG CATCHER TECHNOLOGY IN VILLA MARÍA DEL TRIUNFO - LIMA, PERÚ

Recibido 08/12/2025
Aceptado 19/05/2026

IMPLEMENTACIÓN DE UN SISTEMA PASIVO DE DESHUMIDIFICACIÓN BASADO EN LA TECNOLOGÍA DEL ATRAPANIEBLAS EN VILLA MARÍA DEL TRIUNFO - LIMA, PERÚ

IMPLEMENTAÇÃO DE UM SISTEMA PASSIVO DE DESUMIDIFICAÇÃO BASEADO EM TECNOLOGIA DE CAPTURA DE NÉVOA EM VILLA MARÍA DEL TRIUNFO - LIMA, PERÚ

Milagros Delgado-Peña
Arquitecta
Egresada Carrera de Arquitectura, Facultad de Ingeniería
Universidad Tecnológica del Perú
Lima, Perú
https://orcid.org/0009-0004-4678-0919
U17205052@utp.edu.pe

Alonzo Cardenas-Vera-Pinto (Autor de Correspondencia)
Arquitecto
Egresado Carrera de Arquitectura, -Facultad de Ingeniería
Universidad Tecnológica del Perú
Lima, Perú
https://orcid.org/0009-0006-5707-4475
U17102967@utp.edu.pe

Richard Valdivia-Sisniegas
Magíster de Estudios Avanzados en Arquitectura y Desarrollo Sostenible
Docente y Asesor del programa de Titulación, Carrera de Arquitectura
Universidad Tecnológica del Perú
Lima, Perú
https://orcid.org/0000-0003-0783-6831
C19165@utp.edu.pe

CC BY SA

ABSTRACT

In Lima (Peru), homes in high-relative-humidity environments face unfavorable living conditions, with surface condensation and structural deterioration when indoor RH exceeds 65%. In this context, this research evaluates the efficiency of the DESHUME passive dehumidification prototype in a highly saturated environment, such as the hills of Villa María del Triunfo (692 meters above sea level), where temperatures reached 14.04°C, and RH was 100%. The quasi-experimental, in situ methodology was based on the analysis of meteorological records (2020-2024) and the materials' technical characteristics. Validation was carried out by monitoring indoor and outdoor hygrothermal variables for 72 hours in 1:2 and 1:1-scale modules, incorporating fog-collecting technology and the Venturi effect in their design to remove water mass. This resulted in an average reduction of 0.20g/m³ in indoor RH in winter compared to the reference module, demonstrating the system's viability as a hygrothermal regulator for vulnerable high-humidity sectors.

Keywords
humidity, fog, ventilation, coastal housing

RESUMEN

En Lima (Perú), las viviendas ubicadas en entornos de alta humedad relativa enfrentan condiciones desfavorables para la habitabilidad, lo que favorece la condensación superficial y el deterioro constructivo cuando la HR interior supera el 65%. En este contexto, la investigación evalúa la eficiencia del prototipo de deshumidificación pasiva DESHUME en un entorno de alta saturación hídrica, como las lomas de Villa María del Triunfo (692 m.s.n.m.), registrando condiciones de 14,04 °C y 100% de HR. La metodología cuasiexperimental in situ partió del análisis de precedentes meteorológicos (2020-2024) y de las características técnicas de los materiales. La validación se realizó mediante el monitoreo de variables higrotérmicas interiores y exteriores durante 72 h, en módulos a escala 1:2 y 1:1, incorporando en su diseño la tecnología del atrapanieblas y el efecto Venturi para la remoción de masa de agua. Lo que resulta en la reducción promedio de 0,20 g/m³ de HR interior en invierno respecto al módulo referencial, lo que demuestra al sistema como un regulador higrotérmico viable para sectores vulnerables de alta humedad.

Palabras clave
humedad, niebla, ventilación, vivienda en la costa

RESUMO

Em Lima (Peru), as habitações em ambientes com alta umidade relativa enfrentam condições desfavoráveis à habitabilidade, o que favorece a condensação superficial e a deterioração estrutural quando a umidade relativa interna é superior a 65%. Neste contexto, esta pesquisa avalia a eficiência do protótipo de desumidificação passiva DESHUME em um ambiente de alta saturação hídrica: as colinas de Villa María del Triunfo (692 m acima do nível do mar), onde foram registradas temperaturas de 14,04 °C e umidade relativa de 100%. A metodologia quase experimental in situ baseou-se na análise de dados meteorológicos anteriores (2020-2024) e nas características técnicas dos materiais. A validação foi realizada por meio do monitoramento de variáveis higrotérmicas internas e externas durante 72 horas, em módulos nas escalas 1:2 e 1:1, incorporando-se ao projeto a tecnologia de coletores de névoa e o efeito Venturi para a remoção da massa de água. O resultado foi uma redução média de 0,20 g/m³ na umidade relativa do ar interna no inverno em comparação com o módulo de referência, o que demonstra que o sistema é um regulador higrotérmico viável para áreas vulneráveis com alta umidade.

Palavras-chave
umidade, névoa, ventilação, habitação em áreas costeiras

INTRODUCTION

The Metropolitan city of Lima (Peru) is located in the coastal desert of western South America, where the meeting of the Pacific Ocean and the Andes Mountain Range favors the development of the Lomas ecosystem, with fog banks that form along the coast. The presence of fog at 400-1000 m.a.s.l. in this setting is responsible for a high relative humidity (RH) of up to 100% (Moat et al., 2021). During the winter, from June to September, this saturation affects the consolidated urban settlements in these peripheral areas, which expanded by 1,408.32 ha between 2005 and 2017 (Ministry of the Environment [MINAM], 2021). This climatic situation is manifested in the A.H. Ficus del Pedregal, José Carlos Mariátegui Sector, Villa María del Triunfo (VMT), located near the georeferenced boundary as point 10 (N 8659517, E 290903) (MINAM, 2019), where an RH of 100% has been recorded (SENAMHI, n.d. a). By exceeding the recommended standard of 65% relative humidity in a dwelling's occupied spaces (American National Standards Institute [ANSI] / American Society of Heating, Refrigerating and Air-Conditioning Engineers [ASHRAE]. 62.1, 2025), there is a proliferation of mold and bacteria, as well as the degradation of air quality, which represents a health risk for the inhabitants by increasing the prevalence of chronic respiratory conditions (Campos-Vásquez et al., 2025). This environmental problem not only affects the population's habitability due to weather conditions but is also accentuated by the vulnerability of self-builds, evidenced by a predominance of low-durability materials in housing, such as fiber cement roofs or calamine sheets, earth floors, and OSB or triplay walls (Ministry of Housing, Construction and Sanitation, [MVC], n.d.). These are highly hygroscopic materials that tend to absorb excessive moisture from the environment. This unfavorable environment poses an imminent risk to the materials' durability and does not guarantee adequate insulation or hygrothermal comfort (Tejeda Martínez, 2018). Faced with this problem, recent research has proposed strategies for indoor humidity control using passive or hybrid systems, including the integration of innovative architectural components, such as 3D-printed tiles (Posani et al., 2025). Other approaches similarly propose hybrid ventilation systems with energy recovery for dehumidification (Chen et al., 2023). However, these systems require advanced construction layouts, which make their practical implementation in homes difficult. At the same time, as a sustainable alternative, the capture of atmospheric water using fog catcher technology has been widely studied in the literature. Conventional two-dimensional models (fog nets) that use Raschel meshes on slopes have demonstrated high collection efficiency in arid ecosystems (Ismail & Go, 2021; Qadir et al., 2018). Recently, geometric innovations have been explored, including fog-catcher cylinders for greater wind resistance (Kanooni & Kohan, 2024) and vertical-thread fog harps that improve drainage (Shi et al., 2018). However, despite proven advances in their performance, these devices are installed predominantly as autonomous infrastructure outside living spaces. Thus, a gap remains in the literature regarding the direct integration of this technology into the building. Consequently, this research evaluates the regulation of the absolute humidity (AH) expressed in (g/m^3) by means of a passive dehumidification system that integrates the fog catcher's technology and the Venturi effect, applied to a standard housing module located in the study area.

METHODOLOGY

The research adopted an experimental quantitative approach, using a quasi-experimental design and an in situ comparative evaluation method, with a descriptive and comparative scope. The project aims to reduce internal humidity in a house by implementing a passive dehumidification system. First, areas with the highest fog concentration were identified to define the study area. Later, once located, photographic registration forms were used to determine the characteristics of the dwellings. An analysis of meteorological data from the last five years' winter period was also carried out, along with a study of the materials' thermal performance. In this way, ventilation and collection principles were applied, including the Venturi effect, wind collectors, and fog-catcher technology. Also, to determine the range of habitability and evaluate the prototype's impact, hygrothermal comfort parameters were established following the international standard ANSI/ ASHRAE 62.1-2025, which serves as the regulatory instrument for evaluating naturally conditioned spaces. The acceptable limit for indoor relative humidity is set at 65%. Complementarily, the thermal performance of the building envelope was analyzed using the guidelines of the Peruvian Technical Standard EM.110. With this, the modeling was designed in AutoCAD (2D) and SketchUp (3D). Subsequently, the effectiveness of the prototype was evaluated by comparing two 1:2-scale models: one as a reference and the other intervened with the prototype at 1:1 scale. The modules' scale was justified for logistical feasibility and methodological rigor; these proportions allowed manual transfer, field assembly, and improved control during experimentation. On the other hand, the prototype was kept at a 1:1 scale strictly due to the physical and constructive characteristics of the Raschel mesh. Subsequently, digital measuring instruments, such as hygrometers and anemometers, were used to collect CSV files with RH (%), temperature (°C), and wind speed (m/s) data, which affected the indoor conditions of both models. Finally, hygrothermal calculation equations were applied to obtain the AH value (g/m^3) and to determine the prototype's efficiency.

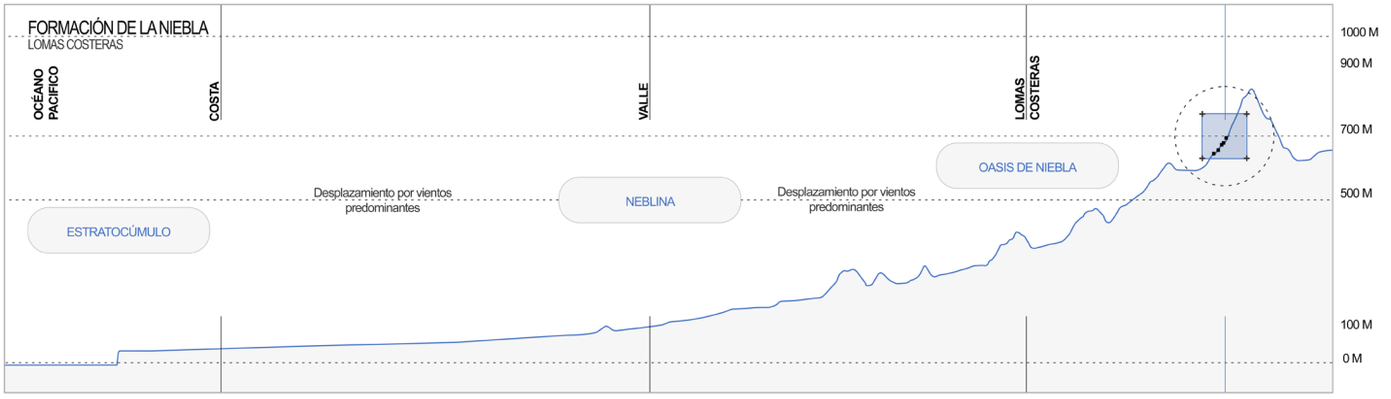


Figure 1. Formation of coastal fog. Source: UNDP (2018).

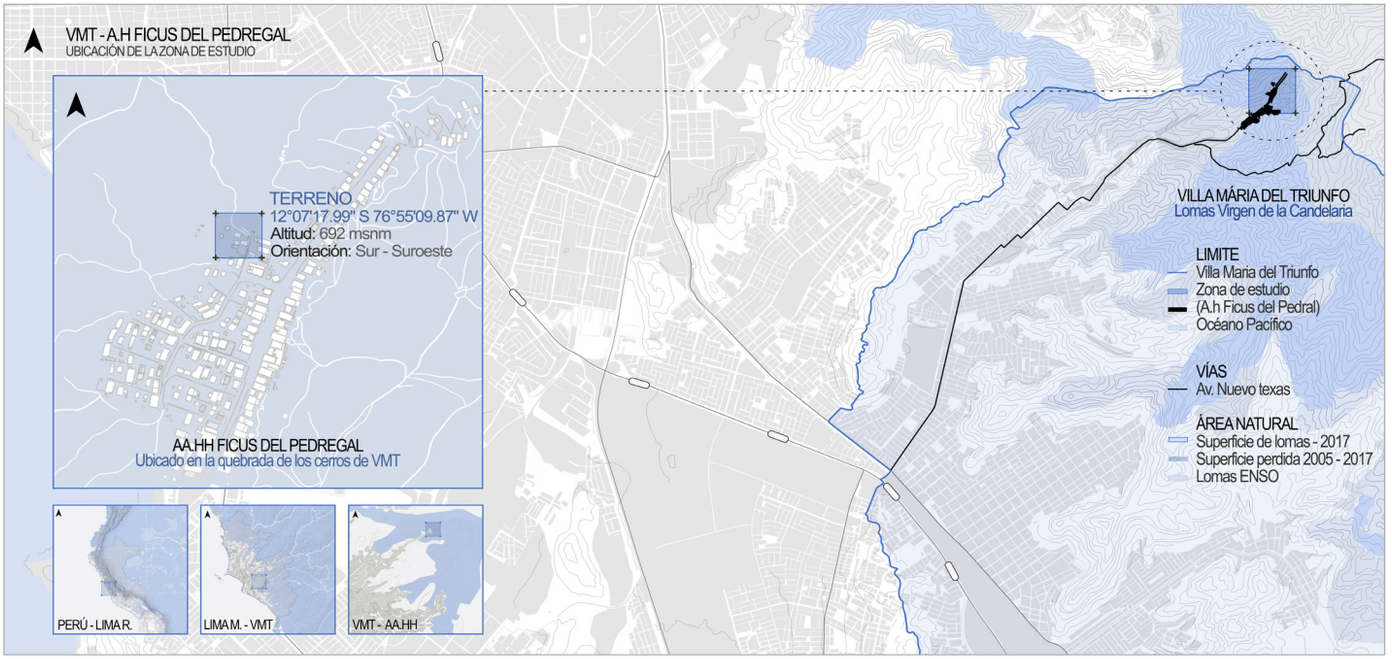


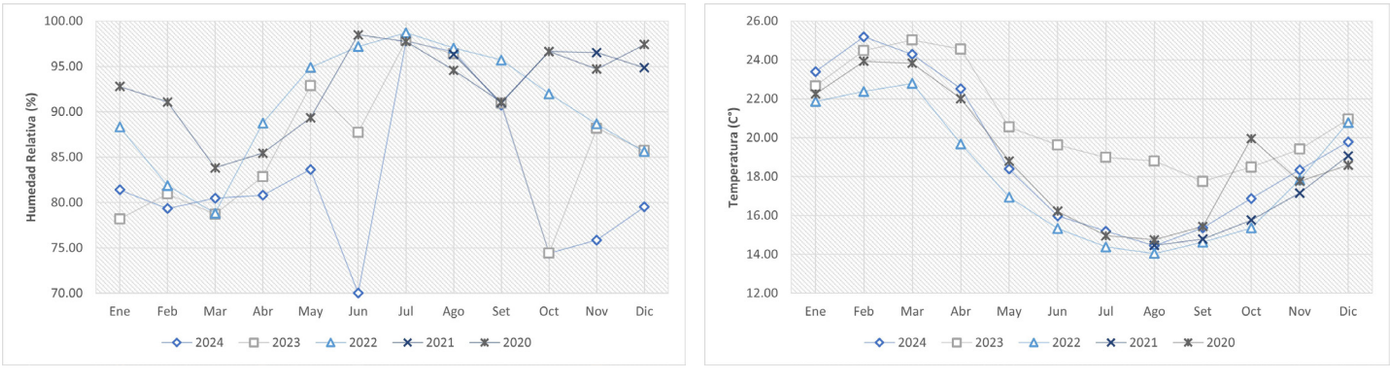
Figure 2. Location of the study area - A.H. Ficus del Pedregal, VMT. Source: Prepared by the authors.

COASTAL FOG FORMATION

The Humboldt Current and the upwelling of cold Pacific waters influence the condensation and formation of coastal fog (United Nations Development Program [UNDP], 2018). When transported by the south and southwest winds towards the foothills of the Andes at altitudes of 400 to 1000 meters above sea level, they create fog banks or oases (Moat et al., 2021) and record RH values of 100% (SENAMHI, n.d, a.) (Figure 1). Humidity, defined as the amount of water vapor in the air, can condense into droplets when the air reaches saturation (Tejeda Martínez, 2018). It is expressed in relative or absolute humidity.

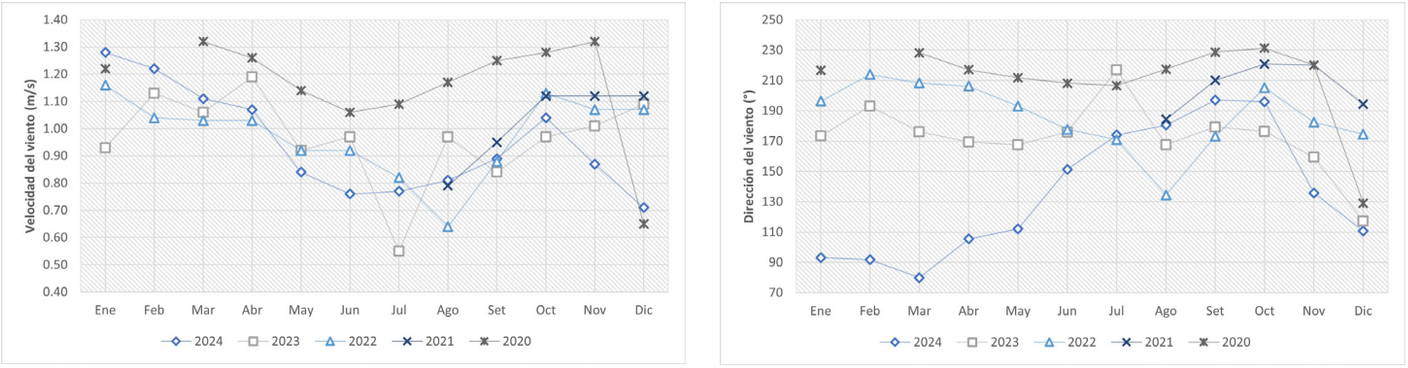
IDENTIFICATION OF THE STUDY AREA

The investigation considered four criteria for the DESHUME project site: 1) Proximity to a coastal hill, 2) Humidity present in the atmosphere, 3) Altitude oscillating from 400 to 1000 meters above sea level, and 4) Orientation perpendicular to the prevailing winds. Therefore, the selected urban area is the A.H. Ficus del Pedregal, José Carlos Mariátegui sector, near the Virgen de la Candelaria Hills, in the district of VMT (MINAM, 2019) (Figure 2). The study area is located at 692 m.a.s.l. (12°07'17.99" S; 76°55'09.87" W), facing the prevailing winds and has fog banks that reach a 100% RH during the winter.



a) b)

Figure 3. (a) Average relative humidity; (b) Average temperature (2020-2024). Source: SENAMHI (n.d. b)



a) b)

Figure 4. (a) Average wind speed; (b) Average wind direction (2020-2024). Source: SENAMHI (n.d.b).

METEOROLOGICAL DATA

To determine the characteristics influencing fog formation and humidity, 5 years of meteorological data (2020-2024) were collected, obtained from the Automatic Meteorological Station of VMT, 112233, located at 292 m.a.s.l., at coordinates 12°9'59" S and 76°55'12" W (SENAMHI, n.d. b). The station performed continuous monitoring of the variables of relative humidity (%), air temperature (°C), wind speed (m/s), and wind direction (°); and the data were recorded with a continuous hourly frequency in CSV files. The records obtained were processed into monthly average values, which were subsequently checked interannually to obtain a final average value.

RELATIVE HUMIDITY AND TEMPERATURE

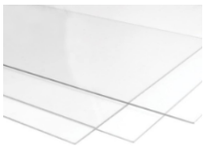
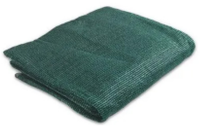
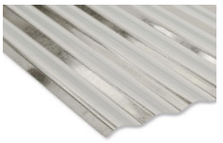
The RH (%) data recorded during the winter of 2020 to 2024 indicate that environmental values exceed the standards, reaching up to 100% (Figure 3a). Also, during the months from June to September, the record of monthly average temperatures for the five years evaluated shows that the lowest temperatures occur in August, at 14.04 °C (Figure 3 b).

WIND SPEED AND DIRECTION

In the winter months of the analyzed period, average speed values showed a progressive increase, reaching a maximum of 5.5 m/s and a minimum of 0.00 m/s, with an average of 0.89 m/s (Figure 4a). The wind direction is measured in degrees relative to true north (0°). In this sense, the predominant direction during the winters of 2020 to 2024 was from the south -southwest, with an average of (≈186.25°) (Figure 4, b).

THERMAL PROPERTIES OF THE MATERIALS

The construction properties of the houses were recorded using photographic record forms. Subsequently, an analysis of the materials' thermal characteristics (Table 1) was carried out to determine their insulating capacity, to consider these conditioning factors in the modules (1:2), and to ensure greater efficiency of the prototype (1:1). For this, the performance (Equation 1) and insulation capacity (Equation 2) were evaluated against the predominant climatic aspects of the study area. The city of Lima was identified in Bioclimatic Zone 1: Coastal Desert. Then, the materials were classified by construction system, and their compliance with the

Properties	Triplay	Acrylic	Raschel Mesh	Metallic calamine
Materials used				
Construction system	Wall	Opening	-	Roof
Dimension (m)	2.44x1.221[1]	1.83x1.221[1]	4.20 x 1.001[1]	3.60x0.801
Thermal Conductivity (λ)	0.14 W/°Cm2[2]	0.200 W/° Cm2[2]	-	0.14 W/°Cm2[2]
Thermal Resistance (R)	0.28 m²°C/W	0.17 m²°C/W	-	0.21 m²°C/W
Thermal Transmittance (U)	3.57 W/m°C	5.88 W/m°C	-	4.76 W/m°C
Moisture Content (%)	5-8	-	-	-
Composition of the Film	Kraft paper+phenolic resin	-	HPPE-UV	Galvanized steel+Zinc
Surface coverage (%)	100	100	50	-
Water vapor permanence (μ)	50	-	-	-
Waterproofing (Approved/ Rejected)	Low	Approved	-	Approved

1 Standard commercial format, 2 Obtained from the EM Technical Standard 110.

Table 1. Technical characteristics of the materials. Source: Prepared by the authors.

maximum permissible thermal transmittance values was evaluated in accordance with the EM.110 Technical Standard (MVCS, 2016).

$$U = 1 / Rt. \quad \text{(Equation 1)}$$

$$Rt = e / \lambda \quad \text{(Equation 2)}$$

Triplay's hygrothermal properties indicate low resistance to vapor entry (μ≈30-50), facilitating the diffusion of moisture into its fibers. This permeability, combined with an RH of more than 65%, creates critical conditions for pathologies such as absorption swelling and fungal colony proliferation. Therefore, this envelope requires a varnish coating to counteract the wooden panel's absorbency. Similarly, metallic calamine, despite its corrosion-resistant zinc coating (90g/m²), has high transmittance and thermal conductivity, allowing heat or cold to pass through without forming a thermal buffer. This shows that the predominant materiality of the houses performs poorly as an insulator in the face of environmental conditions, thereby influencing indoor humidity levels.

CONFIGURATION OF THE PROTOTYPE

Natural or passive ventilation is based on two principles that mobilize the air by natural forces within a room (Saber et al., 2021). One of them is the cross-ventilation generated by the wind (Al-Shamkhee et al., 2022). In the design of passive ventilation systems, the Venturi effect enables air movement without mechanical means (Venturi, 1797). Additionally, Bernoulli's principle reports that the pressure of a fluid decreases as its velocity increases (Suárez et al., 2021). According to this, several studies show that, in order to guarantee the continuity of the air flow, the reduction in the cross-section in a duct (Venturi effect) can accelerate the local wind sufficiently to generate a negative pressure zone that induces the continuous suction of the air (Zhang et al., 2021), maximizing natural ventilation rates (Blocken et al., 2011) (Figure 5, a). This principle was adapted to the design to favor the entry of external air and encourage internal circulation. Thus, the duct of the prototype comprises three successive sections, (i) an inlet section, with a convergence angle of 73° where the air enters at high pressure; (ii) a throat or core section, where the reduction in dimensions concentrates the flow and generating a low pressure zone; and (iii) an outlet section with a divergence angle of 52°, where the duct recovers its dimensions and the flow returns to high pressure conditions (Figure 5, b). The relationship between the angles of convergence and divergence, as well as between the duct's height and width, proved crucial to optimizing the natural movement of air.

The prevailing wind direction determined the prototype's location. Therefore, the fundamentals of the wind catcher were adapted (Figure 6, a) (Ortego Fernández,

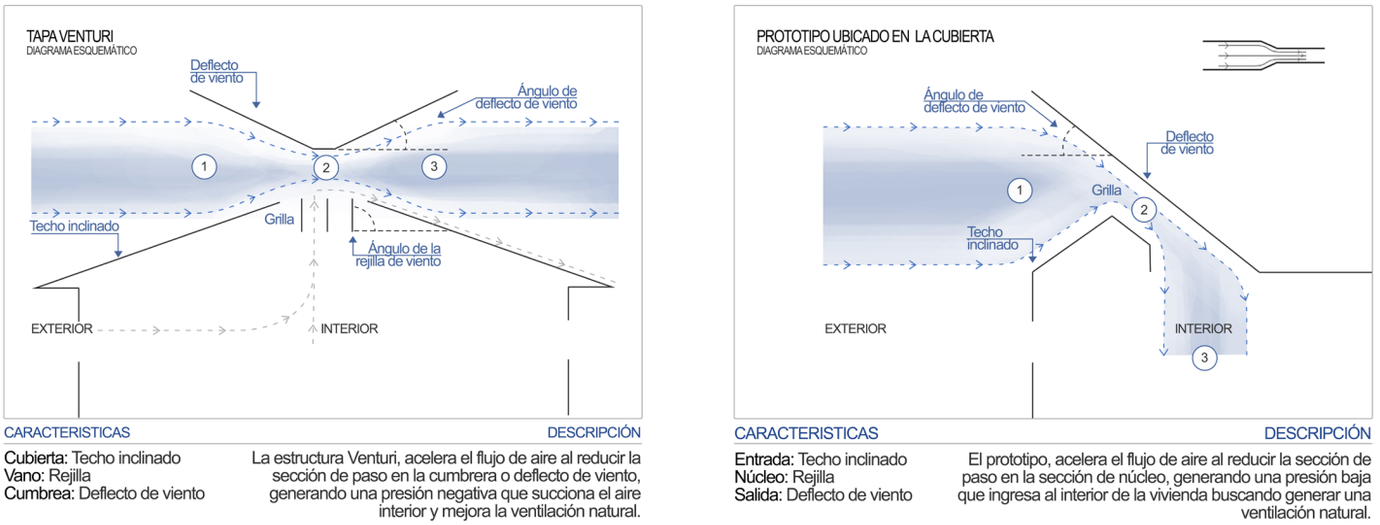


Figure 5. (a) Schematic diagram of the Venturi effect. Source: Zhang et al., 2021; (b) Schematic diagram of the prototype. Source: Prepared by the authors.

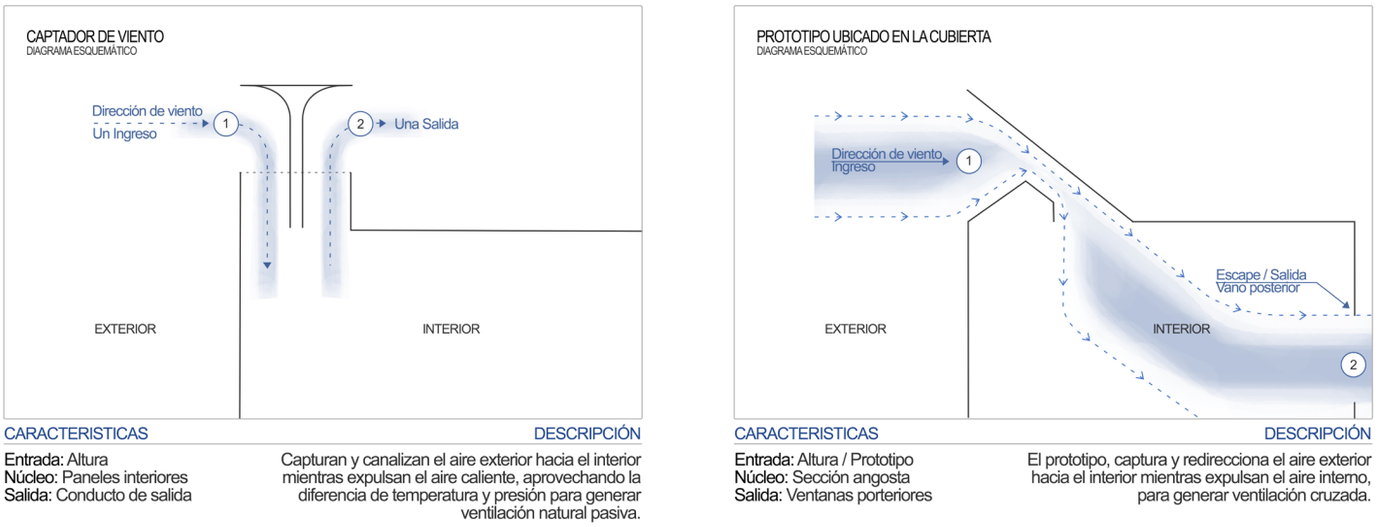


Figure 6. (a) Schematic diagram of wind catcher. Source: Ortego Fernández (2020); (b) Schematic diagram of the prototype. Source: Prepared by the authors.

2020), having a design that seeks to capture and redirect outdoor air currents inside the housing module through a duct that facilitates its entry and distribution. In this way, the configuration of the prototype allows the capture and introduction of external airflow into the house, encouraging internal circulation and cross-ventilation, which promotes the removal of indoor humidity (Figure 6, b).

The design of the prototype not only aims to avoid the accumulation of moisture through ventilation, but also seeks to capture the air coming from the outside, with an RH close to 100%, introducing it with reduced levels, after being mechanically filtered by the meshes, thus obtaining a passive dehumidifying system (Tejeda Martínez, 2018). Therefore, the two-dimensional fog catcher technology is incorporated (Qadir et al., 2018), recognized as an effective passive solution for water harvesting in arid ecosystems and coastal hills. The physical principle is based on the direct interception of fog composed of microscopic water droplets suspended in the air, with diameters ranging from 1 to 30 microns (Márquez Robles, 1993). When the wind pushes this saturated mass against a perpendicularly installed porous surface, the droplets impact the filaments, coalescing and falling by gravity (Ismail & Go, 2021) (Figure 7, a). Thus, the mesh acts as a physical filter that extracts liquid water mass from the airflow before it enters, thereby actively reducing its absolute humidity. The efficiency of this water removal

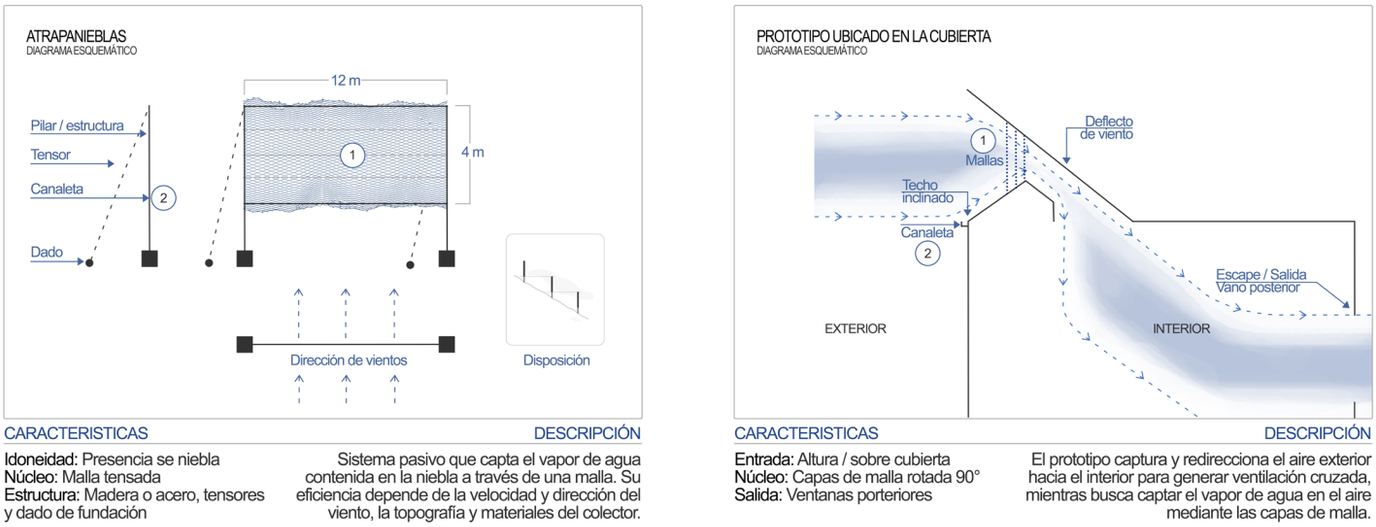


Figure 7. (a) Schematic diagram of the fog catcher. Source: Di Bitonto (2019); (b) Schematic diagram of the prototype. Source: Prepared by the authors.

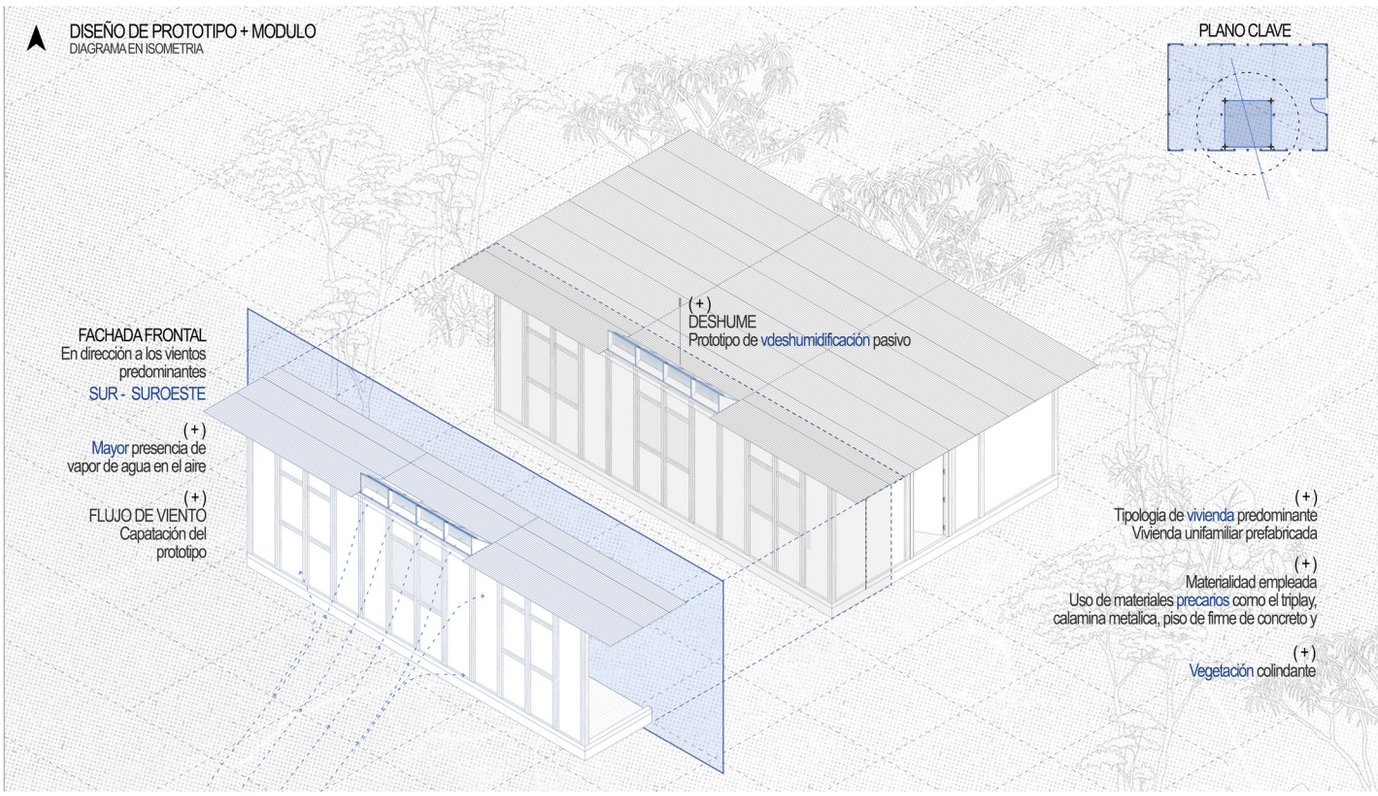


Figure 8. Implementation of a prototype in a dwelling. Source: Prepared by the authors.

is directly proportional to the size of the collecting surface, measured as liters collected per square meter per day (L/m²/day) (Ghiasi, Aslani & Alisoltani, 2025). This makes it possible to capture at least 1 L/m²/day of installed mesh. (Vásquez-Ramírez, Cieza-León & Cieza-León, 2020). In this sense, to maximize airflow impact given the prototype's smaller front opening area (0.24 m²) and dehumidify an interior volume of 1.82 m³, the design compensates for this limitation by increasing the net capture area. The core consists of three layers of polyethylene Raschel mesh in parallel, spaced 4cm apart, and alternating

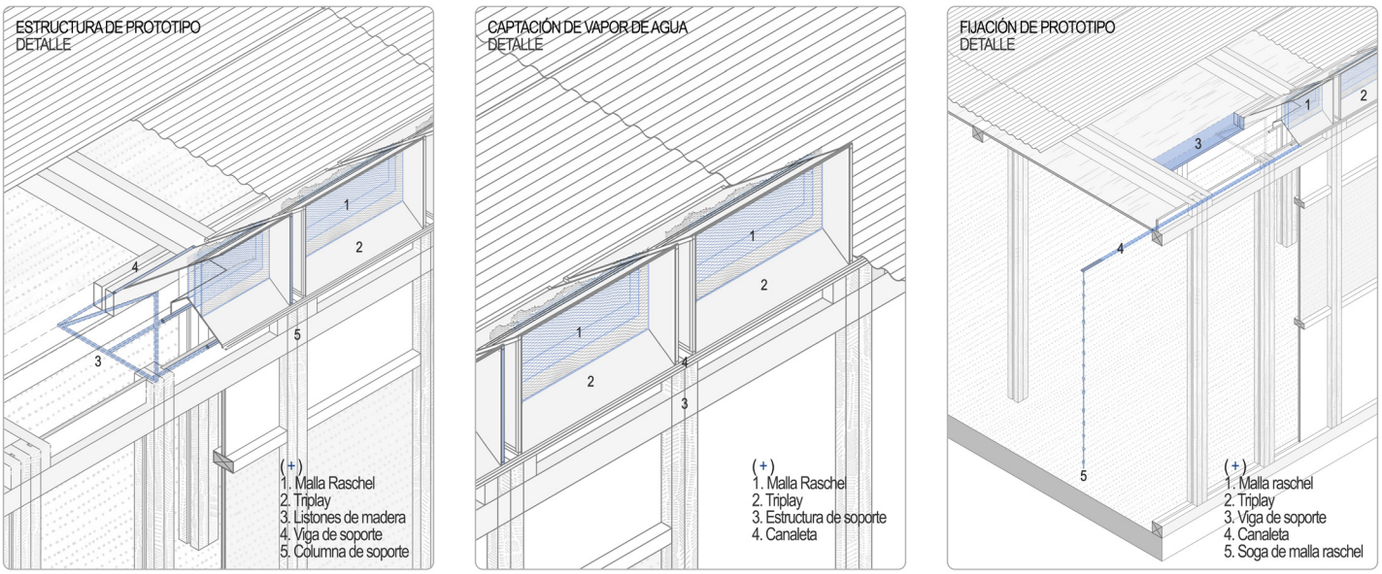


Figure 9. (a) Detail of the installation; (b) Detail of the capture; (c) Detail of the redirection of the collected water. Source: Prepared by the authors.

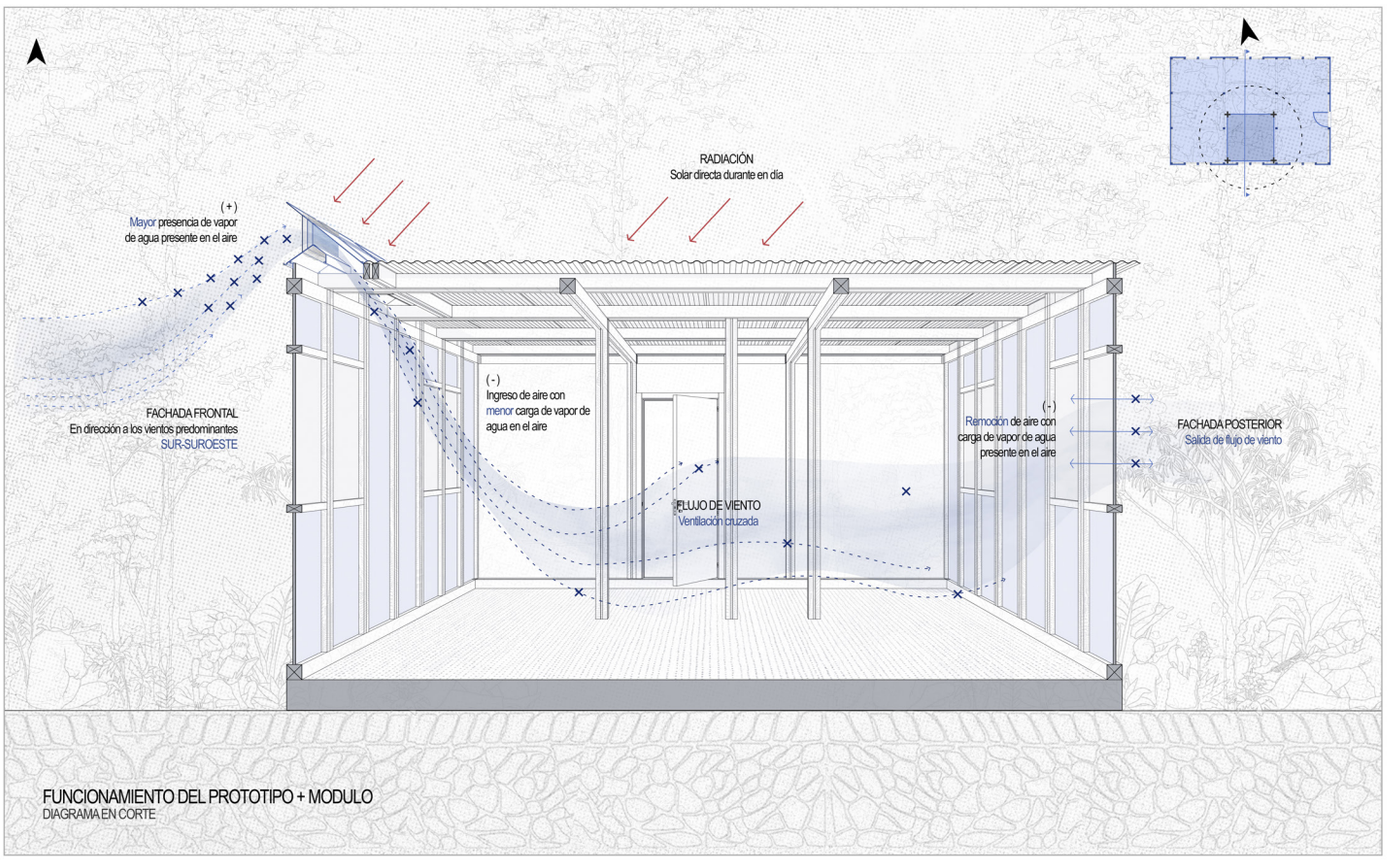


Figure 10. Operation of the DESHUME prototype in a dwelling. Source: Prepared by the authors.

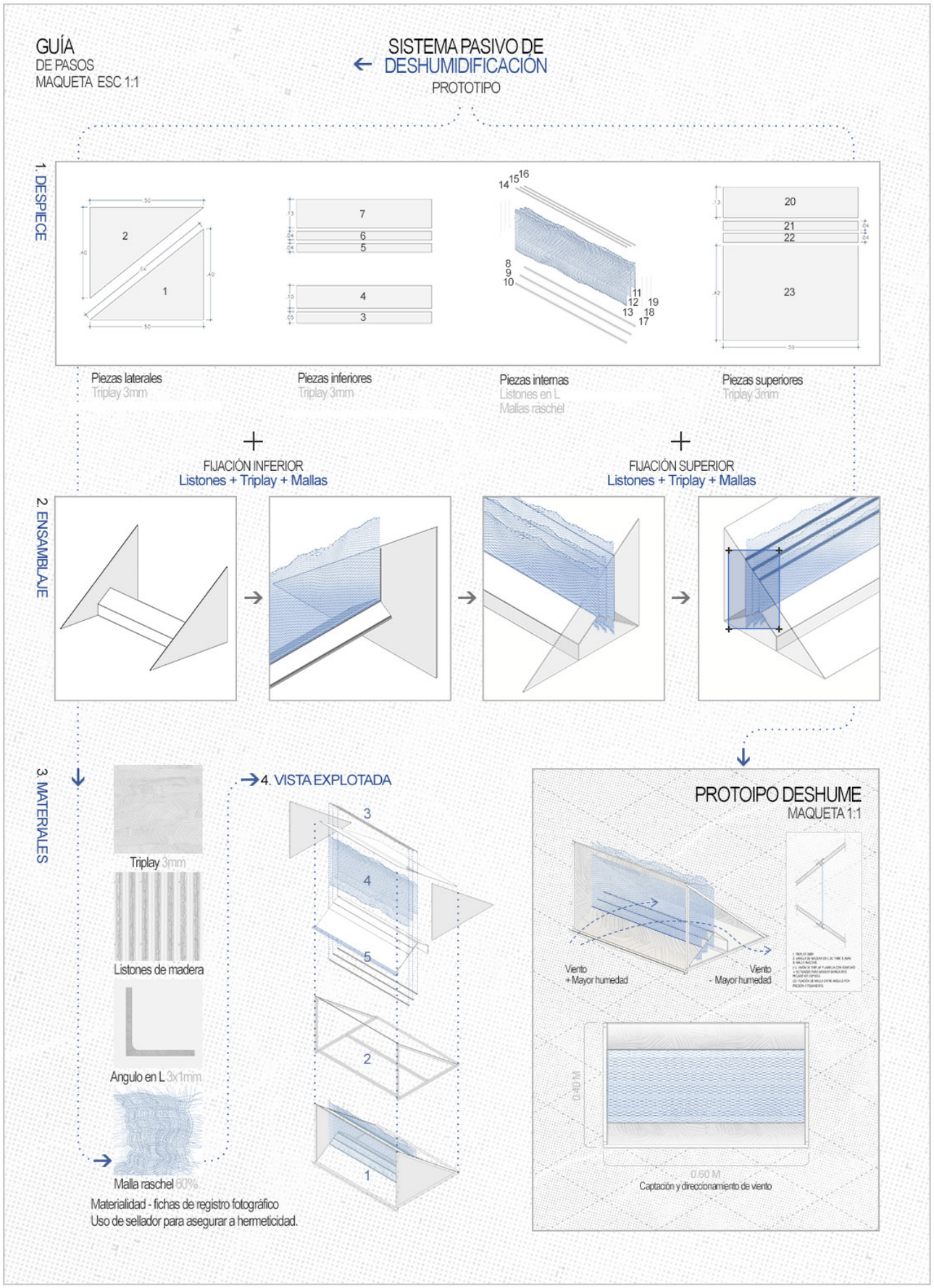


Figure 11. Assembly of the prototype. Source: Prepared by the authors.



Figure 12. Photographic record of the Prototype's assembly. Source: Prepared by the authors.

horizontally and vertically to avoid overlap (Figure 7 b). This configuration densifies the moisture-collecting surface within a reduced area, considering wind orientation, the optimal shade of 50%-60% (Regalado & Ritter, 2016), and reducing its wear from factors such as radiation. Finally, the captured water is redirected by gravity through an external gutter. In this way, fog-catcher technology is used and enhanced to develop a prototype that efficiently integrates wind, surface area, and humidity.

PROTOTYPE + MODULE DESIGN

A 5.50×8.80 m housing module was designed to replicate the characteristics of the study area's typologies (Figure 8). The prototype was installed on the facade, perpendicular to the prevailing winds, on the wooden structures (Figure 9a), which serve as supports to ensure its proper installation and operation. This arrangement allows the three layers of mesh to intercept water vapor in the wind flow (Figure 9, b), redirecting the captured water towards a gutter (Figure 9, c), and, in turn, the pressure generated by the Venturi effect allows the airflow to enter the house. In this way, the prototype facilitates natural ventilation and reduces the accumulation of indoor humidity, ultimately allowing its exit through the rear openings (Figure 10).

ASSEMBLY OF THE PROTOTYPE

The assembly of the prototype at 1:1 scale (Figure 11) involved dismantling its components, taking into account the selected materials and the system's construction logic. An adhesive and activator kit for wood was used in this process, enabling fast and efficient attachment. It was started by joining the side pieces (1) and (2) with the lower ones (3) and (4). Subsequently, the three pairs of lower L-angles (8, 9, and 10) were attached at one end of pieces (4) and (7), and at both ends of pieces (5) and (6). Then, the meshes were placed successively: (11) between (4-5), (12) between (5-6), and (13) between (6-7). The pieces that exert pressure on each mesh were simultaneously adhered to sides (1) and (2), thereby ensuring their attachment. In the next step, the Raschel meshes (11, 12, and 13) were tightened and fixed to the sides (1) and (2) using 3×1mm rods (17, 18, and 19) on both sides, which were pressed between these and the side pieces. Then, the three pairs of upper L-angles (14, 15, and 16) were adhered at the ends of pieces (20) and (23), and at both ends of pieces (21) and (22). Then, the meshes were arranged in sequence: (13) between (20-21), (12) between (21-22), and (11) between (22-23), and secured to sides (1) and (2). Finally, the joints were sealed with Sikaflex-11FC adhesive to ensure the prototype's tightness (Figure 12).

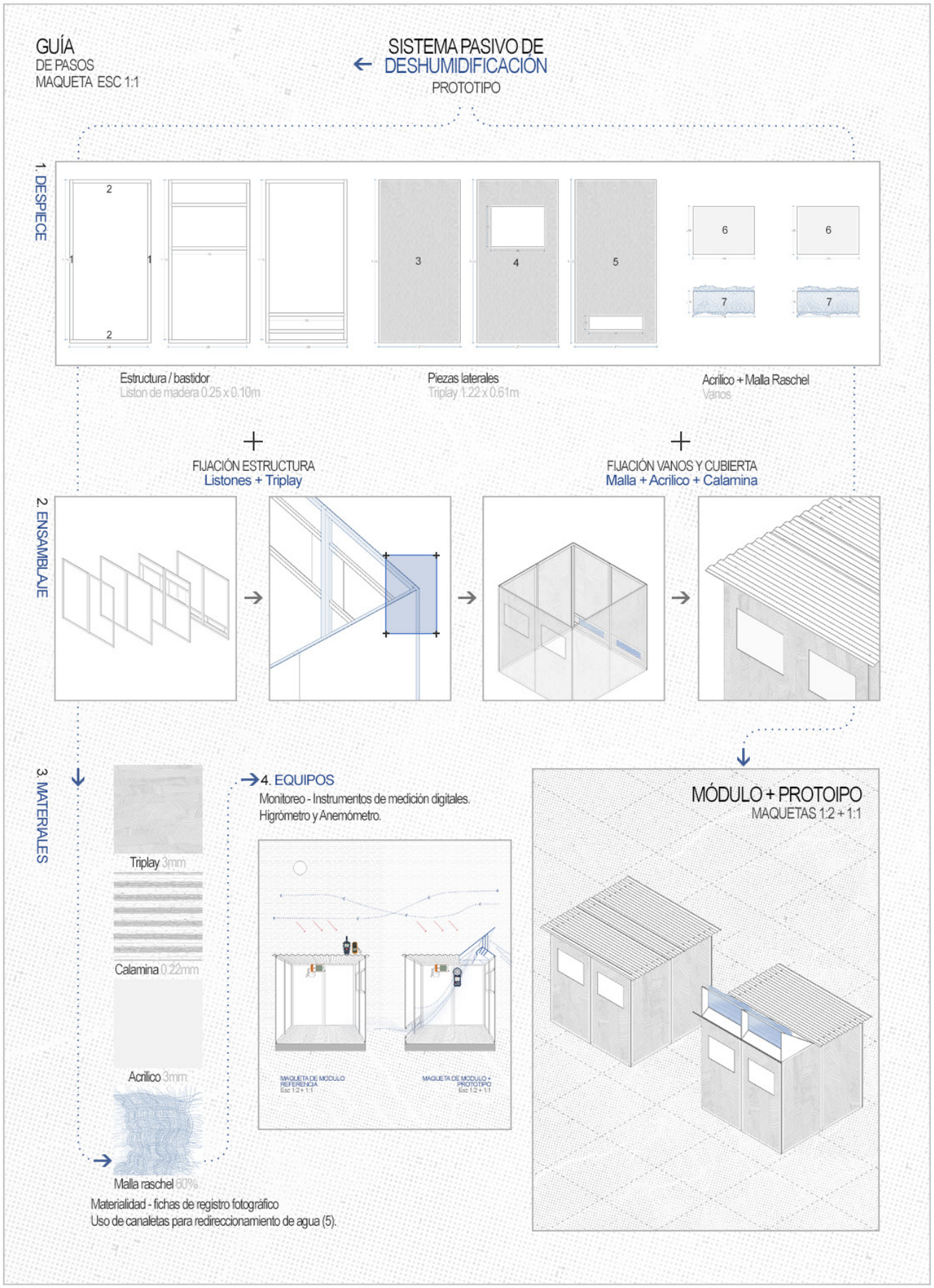


Figure 13. Assembly of the module. Source: Prepared by the authors.



Figure 14. Photographic record of the module's assembly. Source: Prepared by the authors.

ASSEMBLY OF THE MODULE

Subsequently, from a section of the house's front facade, two 1:2-scale models were set up to optimize experimental control in terms of resources, dimensions, and constructability, and to ensure the representativeness of the modules for the study area's climatic conditions. The assembly began with the arrangement of 16 wooden slats (1) and (2), forming 8 frames of 1.22×0.61m, each structured by two slats of both types. Next, 1.22×0.61m (3)(4)(5) Triplay plates were fixed on the 8 frames: two complete pieces formed a side wall. A span of 0.30×0.40m was made on the front wall in each piece (4), and finally, on the back wall, a smaller span of 0.10×0.40m (5) in a single piece. The front spans were covered with 3mm acrylic plates (6), and the back with a layer of Raschel mesh (7). Then, the walls were joined, sealing possible openings with Sikaflex-11FC adhesive to ensure greater tightness. 0.22 mm metal calamine was used for the roof and secured to the structure with nails; the remaining openings were also sealed to prevent leaks. In this way, the assembly of the module and prototype is completed (Figure 13) (Figure 14).

MONITORING AND DATA COLLECTION

During monitoring, the 1:2-scale modules remained unoccupied to control variables such as humidity sources from internal activities. This delimitation made it possible to isolate the performance of the DESHUME system from external climatic conditions and its interaction with the envelope materials, without anthropogenic interference. Likewise, data collection took place after installing the 1:2-scale models onsite, with only one incorporating the 1:1 prototype. Measuring equipment was installed both inside and outside; RH, temperature, and wind speed data were recorded at 15-minute intervals for 3 consecutive days. The temperature and RH were recorded by an Elitech GSP-6 hygrometer inside and a Benetech GT1368 outside. Likewise, the wind speed was recorded with a Wintact WT87B anemometer inside at a height of 1m and 0.50m from the front wall, and with a Benetech GM816 outside. The instruments operated within their respective factory calibration, with very small technical error margins: the inner hygrometer has an accuracy of ±0.5°C and ±3% RH; the outer hygrometer has an accuracy of ±1.5°C and ±5.0% RH; and both anemometers have an operating speed error margin of ±5%. To ensure the representativeness of the hygrothermal conditions, the indoor anemometer was located at 1.00m height, considering comfort and ventilation criteria (Zhai et al., 2015), which determine a range of 1.00m to 1.10m as suitable for evaluating the airflow in the human occupation zone (torso or head

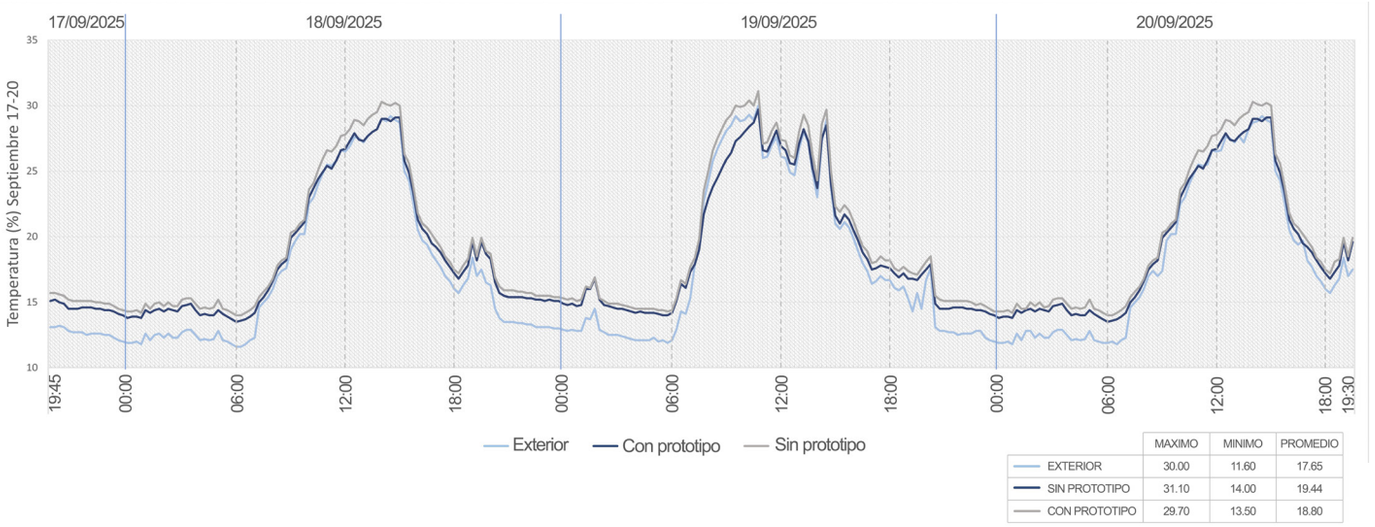


Figure 15. Temperature record - VMT, 2025. Source: Prepared by the authors.

level). Likewise, the instrument was spaced 0.50m from the front wall to avoid measurement bias introduced by thermal transfer and the envelope boundary layer. Finally, the outdoor measurement was performed at a 1.20m SNPT in a clear area to record the unobstructed ambient airflow.

DATA ANALYSIS

Subsequently, a hygrothermal calculation was performed using the Magnus-Tetens approximation (Vaisala, 2013) to convert temperature (°C) and relative humidity (%) into absolute humidity (g/m³). The saturation vapor pressure Pws in hPa was calculated first (Equation 3) and then the actual vapor pressure Pw in hPa (Equation 4).

$$P_{ws}(T) = A \cdot 10^{\frac{m \cdot T}{T+T_n}} \quad (\text{hPa}) \qquad \text{(Equation 3)}$$

$$P_w = P_{ws} \cdot \frac{RH}{100} \quad (\text{en hPa}) \qquad \text{(Equation 4)}$$

Also, to determine the AH (Equation 5), it was required to convert the temperature from °C to °K (Equation 6) and the actual vapor pressure Pw from hPa to Pa (Equation 7), obtaining values in g/m³. This information enabled the comparison of the data collected from the reference module with that from the intervened module and, in turn, validated the effectiveness of the DESHUME system.

$$\boxed{A = C \cdot \frac{P_w}{T}} \quad (\text{g/m}^3) \qquad \text{(Equation 5)}$$

$$T_K = T(^\circ\text{C}) + 273.15 \qquad \text{(Equation 6)}$$

$$1\ \text{hPa} \times 100\ \text{Pa} \qquad \text{(Equation 7)}$$

Then, using the temperature, wind speed, and AH data, comparative tables were prepared for the 3 measurement moments.

RESULTS AND DISCUSSION

The outdoor temperature varied widely between 12°C and 30°C, with an average of 17.7°C. In comparison, the indoor temperature of the intervened module averaged 18.8°C, slightly lower than the reference (19.4°C), indicating a slight thermal damping effect. The nighttime temperatures ranged from 13.5°C to 15.2°C in the prototype and from 14.2°C to 15.7°C in the reference (Figure 15).

When comparing the hygrothermal comfort band (30%-60%) based on the ANSI/ASHRAE 62.1-2025 Standard and the RNE EM.110, the intervals in which indoor environments achieve comfortable conditions are shown (Figure 16). The time spent in the comfort range during the control was 3 days: Outside (13.5 h), Without prototype (19.75 h), and With prototype (18.5 h).

The outdoor AH exceeded the standards, averaging 12g/m³. The module operated with the DESHUME prototype showed a slight reduction to 10.98g/m³; while the reference module indicated 11.18g/m³. The most noticeable variation was observed in the mornings, with 14.41g/m³ for the prototype compared

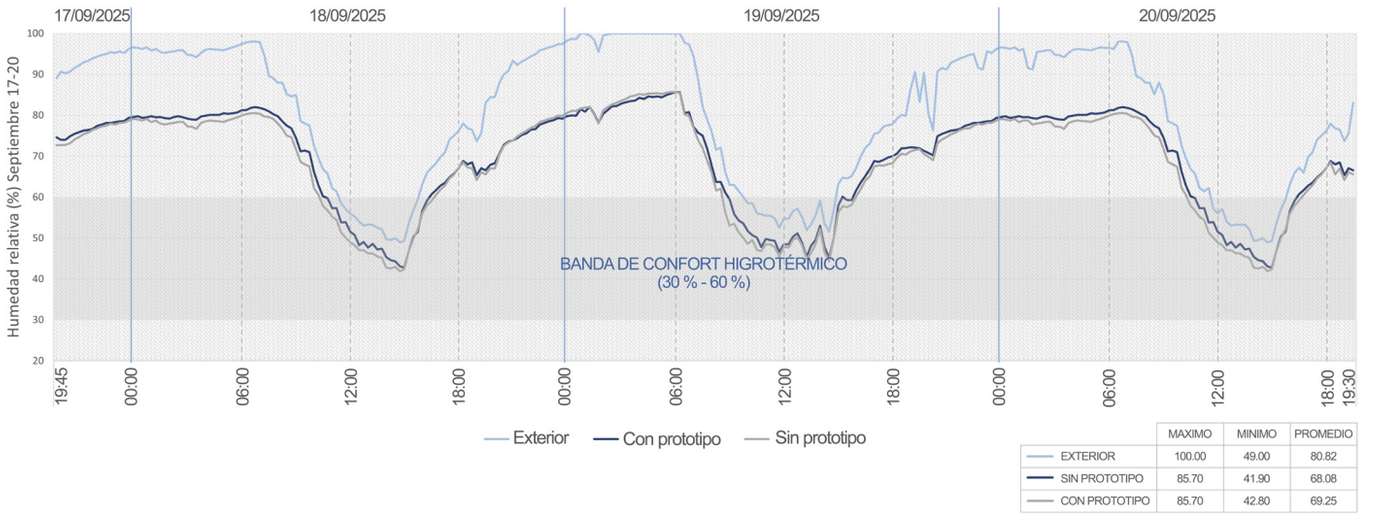


Figure 16. Relative Humidity record - VMT, 2025. Source: Prepared by the authors.

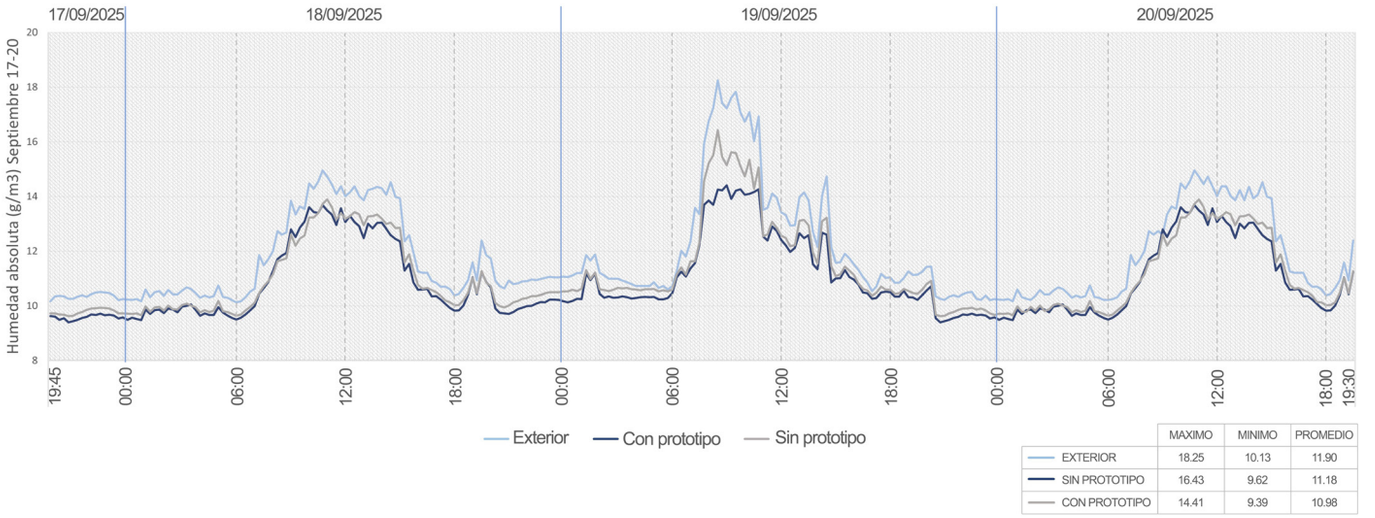


Figure 17. Absolute Humidity record - VMT, 2025. Source: Prepared by the authors.

to 16.43g/m³ for the reference module, indicating a reduction of 2.02g/m³ (Figure 17).

The average outdoor wind speed was 0.44 m/s, with a peak of 2.1 m/s, whereas indoors the anemometer did not record any airflow (Figure 18).

Variations were evident between the variables of absolute humidity (g/m³), wind speed (m/s), and temperature (°C), which reflect internal differences in both modules. The prototype recorded an average of 10.98g/m³ of indoor AH during the study days, which represents a reduction of 0.20g/m³ compared to the reference module (11.18g/m³); they have capture peaks of 2.02g/m³ (12.3%) during the daytime hours and 0.23 g/m³ (2.4%) during the night hours. Although the anemometer did not record measurable indoor wind, these variations indicate that the system functions as a passive regulator of the vapor load by condensation and interception in the Raschel meshes. The decrease in temperature in the prototype module suggests a slight exchange with colder outside air or lower thermal retention. Overall, the prototype demonstrates partial efficiency under weak wind conditions. At this point, its potential as a passive hygrothermal control device through collection stands out, depending on the geometry and the availability of ambient airflow.

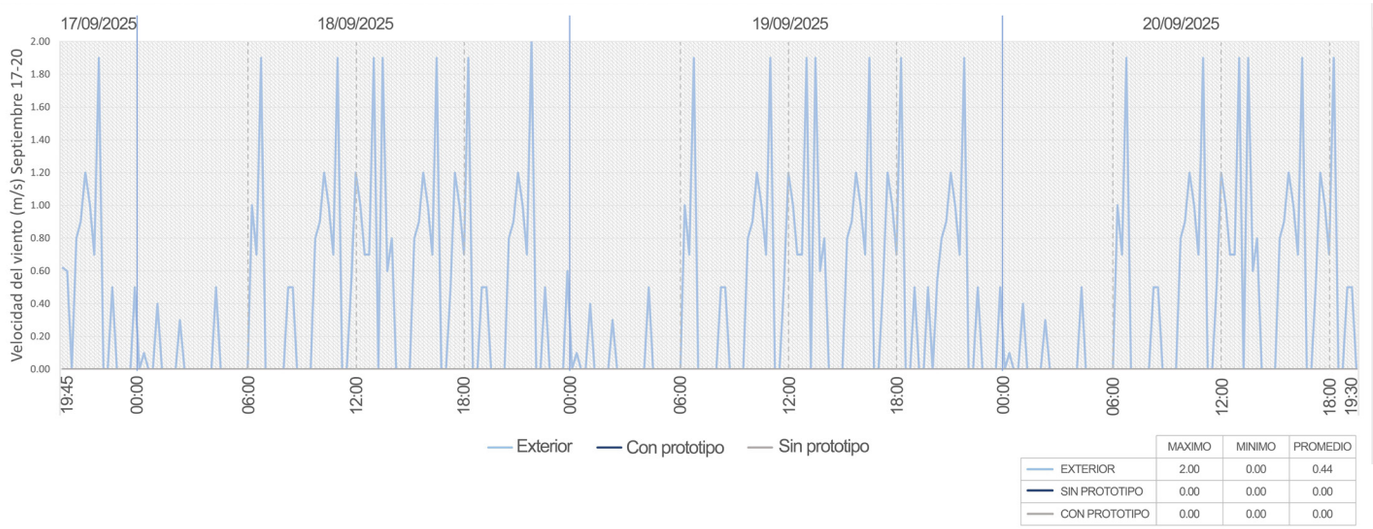


Figure 18. Wind speed record - VMT, 2025. Source: Prepared by the authors.

CONCLUSIONS

The prototype met the main objective of serving as a passive dehumidification strategy, using a modular, easily assembled system conceived for use in homes without requiring major interventions in high-humidity areas. Although the reduction in AH was minimal (1.79%), the prototype demonstrated hygrothermal improvement as a passive system, indicating its potential as a sustainable alternative. Although a slight increase in RH was recorded due to the decrease in indoor temperature, the dehumidification achievement is not invalidated, since a mass of water was removed. An average reduction of 0.20g/m^3 in AH was observed relative to the reference modulus.

The performance of the system is validated by comparing it with the related literature: unlike the reactive storage mechanism of other passive systems that attenuate up to 12% RH at 23°C, in which 2.47g/m^3 of HA is reduced (Zhang, Yoshino & Hasegawa, 2012), DESHUME achieves an active removal of AH (0.20g/m^3) under minimum temperatures and critical saturation conditions (100%RH), by overcoming the dependence on the damping capacity of the construction materials. In addition, when compared with complex solutions, such as the hybrid system (Chen et al., 2023), which reports 5g/m^3 reductions, DESHUME achieves consistent AH removal with a fully passive system, establishing itself as an appropriate strategy for self-construction. However, its performance requires future studies on the mesh's durability under UV exposure and mechanical wind pressure, as well as on the variability of performance with respect to its orientation to prevailing winds.

On the other hand, the Venturi effect did not reduce AH, whereas the moisture retention established by the three layers of mesh predominated. This strategy addressed the reduction in the fog catcher's catchment area and slowed the airflow.

Among the limitations, it can be said that the system's components were not evaluated independently (the geometric sensor without the meshes present), so the specific contribution of the aerodynamic shape versus the mechanical retention of the fabric cannot be broken down. Also, since no Computational Fluid Dynamics (CFD) simulations were performed, it is not possible to accurately estimate the geometry's contribution to the increase in dynamic pressure.

Finally, it is recommended to analyze the relationship between the volume of the 1:2 module (1.82 m^3) and the dimensions of the opening in the 1:1 prototype, whose geometric design allows control of the air pressure and velocity entering the house, as well as the acceleration of the wind's passage. Also, it is suggested to evaluate the behavior of the 1:1 prototype in a real house, for a longer period and in different seasons, using differential pressure sensors or more sensitive anemometers, in addition to considering anthropogenic hygrothermal load factors (breathing and cooking), to evaluate the performance of the system against internal steam sources.

CONTRIBUTION OF AUTHORS CRediT:

Conceptualization, M.N.D.P.; Data Curation, M.N.D.P. and A.L.C.V.P.; Formal analysis, M.N.D.P. and A.L.C.V.P.; Acquisition of financing M.N.D.P. and A.L.C.V.P.; Research, M.N.D.P. and A.L.C.V.P.; Methodology, M.N.D.P. and A.L.C.V.P.; Project management, M.N.D.P. and A.L.C.V.P.; Resources, M.N.D.P. and A.L.C.V.P.; Software. M.N.D.P. and A.L.C.V.P.; Supervision, R.H.V.S.; Validation, M.N.D.P. and A.L.C.V.P.; Visualization, M.N.D.P. and A.L.C.V.P; Writing - original draft, M.N.D.P. and A.L.C.V.P.; Writing - proofreading and editing, M.N.D.P. and A.L.C.V.P.

ACKNOWLEDGMENTS

The authors express their gratitude to the people involved during the experimentation process for their participation, valuable collaboration, and disinterested support in the development of the research. They also extend sincere recognition to the Technological University of Peru for the institutional support provided.

BIBLIOGRAPHIC REFERENCES

Al-Shamkhee, D., Al-Aasam, A. B., Al-Waeli, A. H. A., Abusaibaa, G. Y., & Moria, H. (2022). Passive cooling techniques for ventilation: an updated review. *Renewable Energy and Environmental Sustainability*, *7*(23), 1-16. https://doi.org/10.1051/rees/2022011

American National Standards Institute [ANSI] / American Society of Heating, Refrigerating and Air-Conditioning Engineers [ASHRAE]. (2025). *ANSI/ASHRAE 62.1-2025: Ventilation and Acceptable Indoor Air Quality (Includes ANSI/ASHRAE addenda listed in Appendix Q).* ANISI Webstore. https://webstore.ansi.org/standards/ashrae/ansiashrae622025-2598518?source=blog

Blocken, B., van Hooff, T., Aanen, L., & Bronsema, B. (2011). Computational analysis of the performance of a venturi-shaped roof for natural ventilation: Venturi-effect versus wind-blocking effect. *Computers & Fluids*, *48*(1), 202–213. https://doi.org/10.1016/j.compfluid.2011.04.012

Campos-Vásquez, N., Manturano-Chipana, R. K., & Rabanal-Chávez, E. H. (2025). Causas e Influencia de la humedad en la infraestructura de las edificaciones. *Ciencia y Tecnología*, *24*(2), 27-33. https://doi.org/10.70414/cyt.v24i2.126

Chen, Y., Ozaki, A., Lee, H., Choi, Y., & Arima, Y. (2023). Development of an intelligent envelope system with energy recovery ventilation for passive dehumidification in summer and solar collection in winter. *E3S Web of Conferences*, *396*, 03025. https://doi.org/10.1051/e3sconf/202339603025

Di Bitonto, M. G. (2019). *Oasis productivo: infraestructura de acceso al Parque Pan de Azúcar para la preservación del sector a través de agua de niebla* [Tesis de maestría, Pontificia Universidad Católica de Chile]. Repositorio. https://repositorio.uc.cl/handle/11534/26488

Ghiasi, B., Aslani, Z. H., & Alisoltani, T. (2025). Assessing the feasibility and sustainability of fog water harvesting as an alternative water resource. *Scientific reports*, *15*(1), 19254. https://doi.org/10.1038/s41598-025-03919-3

Ismail, Z., & Go, Y. I. (2021). Fog-to-Water for Water Scarcity in Climate Change Hazards Hotspots: Pilot Study in Southeast Asia. *Global Challenges*, 5(5), 2000036. https://doi.org/10.1002/gch2.202000036

Kanooni, A., & Kohan, M. R. (2024). Fog water harvesting with cylindrical brush. *Scientific Report*s, *14*(1),19679. https://doi.org/10.1038/s41598-024-70637-7

Márquez Robles, J. (1993). Atrapanieblas: una tecnología para la reforestación de las lomas costeras del Perú. *Ingeniería Industrial*, 7(007), 88–98. https://doi.org/10.26439/ing.ind1993.n007.3073

Ministerio del Ambiente [MINAM]. (7 de diciembre de 2019). Decreto Supremo N.° 011-2019-MINAM: Establece el Área de Conservación Regional Sistema de Lomas de Lima. *Diario Oficial del Bicentenario El Peruano. Normas Legales, 5-11*. https://busquedas.elperuano.pe/dispositivo/NL/1834838-3

Ministerio del Ambiente[MINAM]. (15 de agosto de 2021). *Mapa de lomas costeras de Lima Metropolitana*. Sistema Nacional de Información Ambiental [SINIA]. https://sinia.minam.gob.pe/mapas/mapa-lomas-costeras-lima-metropolitana-2021

Moat, J., Orellana-García, A., Tovar, C., Arakaki, M., Arana, C., Cano, A., Faundez, L., Gardner, M., Hechenleitner, P., Hepp, J., Lewis, G., Mamani, J.-M., Miyasiro, M., & Whaley, O. Q. (2021). Seeing through the clouds – Mapping desert fog oasis ecosystems using 20 years of MODIS imagery over Peru and Chile. *International Journal of Applied Earth Observation and Geoinformation*, *103*, 102468. https://doi.org/10.1016/j.jag.2021.102468

Ministerio de Vivienda, Construcción y Saneamiento, [MVCS]. (s.f.). GeoVivienda. Plataforma GIS del Ministerio de Vivienda, Construcción y Saneamiento. https://geo.vivienda.gob.pe/

Norma Técnica EM.110 (2016) [Ministerial Ministerio de Vivienda, Construcción y Saneamiento - MVCS]. Por la cual se establecen los parámetros técnicos de Confort Térmico y Lumínico con Eficiencia Energética. 27 de julio del 2016. https://www.gob.pe/es/i/2619729

Ortego Fernández, I. (2020). Torres de viento. Relectura contemporánea de sistemas energéticos pasivos [Trabajo Fin de Grado, Universidad Politécnica de Madrid]. Repositorio UPM. https://oa.upm.es/57995/

Programa de las Naciones Unidas para el Desarrollo [PNUD]. (16 de mayo de 2018). *Proyecto EbA Lomas: Retos y oportunidades en la conservación de las lomas de Lima Metropolitana*. https://www.undp.org/es/peru/publications/eba-lomas

Posani, M., Voney, V., Odaglia, P., Du, Y., Komkova, A., Brumaud, C., Dillenburger, B., & Habert, G. (2025). Low-carbon indoor humidity regulation via 3D-printed superhygroscopic building components. *Nature Communications*, *16*, 425. https://doi.org/10.1038/s41467-024-54944-1

Qadir, M., Jiménez, G. C., Farnum, R. L., Dodson, L. L., & Smakhtin, V. (2018). Fog water collection: Challenges beyond technology. *Water*, *10*(4), 372. https://doi.org/10.3390/w10040372

Regalado, C. M., & Ritter, A. (2016). The design of an optimal fog water collector: A theoretical analysis. Atmospheric *Research*, *178–179*, 45–54. https://doi.org/10.1016/j.atmosres.2016.03.006

Saber, E. M., Chaer, I., Gillich, A., & Ekpeti, B. G. (2021). Review of intelligent control systems for natural ventilation as passive cooling strategy for UK buildings and similar climatic conditions. *Energies, 14*(15), 4388. https://doi.org/10.3390/en14154388

Servicio Nacional de Meteorología e Hidrología del Perú [SENAMHI]. (s.f. a). *Estaciones meteorológicas.* Datos/ Datos Hidrometeorológicos*.* https://www.senamhi.gob.pe/?&p=estaciones

Servicio Nacional de Meteorología e Hidrología del Perú [SENAMHI]. (s.f. b). *Estadística de la calidad del aire: Estacion 112233.* https://www.senamhi.gob.pe/?p=calidad_del_aire-estadistica&e=112233

Shi, W., Anderson, M. J., Tulkoff, J. B., Kennedy, B. S., & Boreyko, J. B. (2018). Fog harvesting with vertical harps. *ACS Applied Materials & Interfaces*, 10(14), 11979–11986. https://pubs.acs.org/doi/10.1021/acsami.7b17488

Suárez, Á., Dutra, M., Monteiro, M., & Martí, A. C. (2021). El embrollo de Bernoulli: una investigación sobre las concepciones alternativas de los estudiantes en dinámica de fluidos. *Modelling in Science Education and Learning, 14* (2), 17–30. https://doi.org/10.4995/msel.2021.14835

Tejeda Martínez, A. (2018). *La humedad en la atmósfera. Bases físicas, instrumentos y aplicaciones*. Universidad de Colima. http://ww.ucol.mx/publicacionesenlinea/promocion.php?docto=466

Vaisala, O. (2013). Humidity Conversion Formulas*: Calculation formulas for humidity*. (Technical Reference B210973EN-F). https://www.hatchability.com/Vaisala.pdf

Venturi, J. B. (1797). *Recherches expérimentales sur le principe de la communication latérale du mouvement dans les fluides. Houel et Ducros*. Théophile Barrois. https://gallica.bnf.fr/ark:/12148/bpt6k9611865z.textelmage

Vásquez-Ramírez, L., Cieza-León, L., & Cieza-León, D. (2020). Eficiencia de captación de agua con tres tipos de malla atrapanieblas en zonas rurales altoandinas de la sierra norte del Perú. *Revista Ingeniería UC*, 27(3), 319-327. https://servicio.bc.uc.edu.ve/ingenieria/revista/

Zhai, Y., Zhang, Y., Zhang, H., Pasut, W., Arens, E., & Meng, Q. (2015). Human comfort and perceived air quality in warm and humid environments with ceiling fans. *Building and Environment*, 90, 178-185. https://doi.org/10.1016/j.buildenv.2015.04.00

Zhang, H., Yoshino, H., & Hasegawa, K. (2012). Assessing the moisture buffering performance of hygroscopic material by using experimental method. *Building and Environment*, 48, 27-34. https://doi.org/10.1016/j.buildenv.2011.08.012

Zhang, L., Tian, L., Shen, Q., Liu, F., Li, H., Dong, Z., Cheng, J., Liu, H., & Wan, J. (2021). Study on the influence and optimization of the Venturi effect on the natural ventilation of buildings in the Xichang Area. *Energies*, *14*(16), 5053. https://doi.org/10.3390/en14165053